Present Status and Future of DCC Analysis

Tapan K. Nayak* *for the WA98 Collaboration*

M.M. Aggarwal[a], A. Agnihotri[b], Z. Ahammed[c], A.L.S. Angelis[d], V. Antonenko[e], V. Arefiev[f], V. Astakhov[f], V. Avdeitchikov[f], T.C. Awes[g], P.V.K.S. Baba[h], S.K. Badyal[h], A. Baldine[f], L. Barabach[f], C. Barlag[i], S. Bathe[i], B. Batiounia[f], T. Bernier[j], K.B. Bhalla[b], V.S. Bhatia[a], C. Blume[i], R. Bock[k], E.-M. Bohne[i], D. Bucher[i], A. Buijs[l], E.-J. Buis[l], H. Büsching[i], L. Carlen[m], V. Chalyshev[f], S. Chattopadhyay[c], K.E. Chenawi[m], R. Cherbatchev[e], T. Chujo[n], A. Claussen[i], A.C. Das[c], M.P. Decowski[l], V. Djordjadze[f], P. Donni[d], I. Doubovik[e], M.R. Dutta Majumdar[c], S. Eliseev[o], K. Enosawa[n], H. Feldmann[i], P. Foka[d], S. Fokin[e], V. Frolov[f], M.S. Ganti[c], S. Garpman[m], O. Gavrishchuk[f], F.J.M. Geurts[l], T.K. Ghosh[p], R. Glasow[i], S.K. Gupta[b], B. Guskov[f], H.A. Gustafsson[m], H.H. Gutbrod[j], R. Higuchi[n], I. Hrivnacova[o], M. Ippolitov[e], H. Kalechofsky[d], R. Kamermans[l], K.-H. Kampert[i], K. Karadjev[e], K. Karpio[q], S. Kato[n], S. Kees[i], H. Kim[g], B.W. Kolb[k], I. Kosarev[f], I. Koutcheryaev[e], A. Kugler[o], P. Kulinich[r], V. Kumar[b], M. Kurata[n], K. Kurita[n], N. Kuzmin[f], I. Langbein[k], A. Lebedev[e], Y.Y. Lee[k], H. Löhner [p], D.P. Mahapatra[s], V. Manko[e], M. Martin[d], A. Maximov[f], R. Mehdiyev[f], G. Mgebrichvili[e], Y. Miake[n], D. Mikhalev[f], G.C. Mishra[s], Y. Miyamoto[n], D. Morrison[t], D.S. Mukhopadhyay[c], V. Myalkovski[f], H. Naef[d], B.K. Nandi[s], S.K. Nayak[j], T.K. Nayak[c], S. Neumaier[k], A. Nianine[e], V. Nikitine[f], S. Nikolaev[e], S. Nishimura[n], P. Nomokov[f], J. Nystrand[m], F.E. Obenshain[t], A. Oskarsson[m], I. Otterlund[m], M. Pachr[o], A. Parfenov[f], S. Pavliouk[f], T. Peitzmann[i], V. Petracek[o], F. Plasil[g], M.L. Purschke[k], B. Raeven[l], J. Rak[o], S. Raniwala[b], V.S. Ramamurthy[s], N.K. Rao[h], F. Retiere[j], K. Reygers[i], G. Roland[r], L. Rosselet[d], I. Roufanov[f], J.M. Rubio[d], S.S. Sambyal[h], R. Santo[i], S. Sato[n], H. Schlagheck[i], H.-R. Schmidt[k], G. Shabratova[f], I. Sibiriak[e], T. Siemiarczuk[q], B.C. Sinha[c], N. Slavine[f], K. Söderström[m], N. Solomey[d], S.P. Sørensen[t], P. Stankus[g], G. Stefanek[q], P. Steinberg[r], E. Stenlund[m], D. Stüken[i], M. Sumbera[o], T. Svensson[m], M.D. Trivedi[c], A. Tsvetkov[e], C. Twenhöfel[l], L. Tykarski[q], J. Urbahn[k], N.v. Eijndhoven[l], W.H.v. Heeringen[l], G.J.v. Nieuwenhuizen[r], A. Vinogradov[e], Y.P. Viyogi[c], A. Vodopianov[f], S. Vörös[d], M.A. Vos[l], B. Wyslouch[r], K. Yagi[n], Y. Yokota[n], and G.R. Young[g]

[a] *University of Panjab, Chandigarh 160014, India* [b] *University of Rajasthan, Jaipur 302004, Rajasthan, India* [c] *Variable Energy Cyclotron Centre, Calcutta 700064, India* [d] *University of Geneva, CH-1211, Geneva 4, Switzerland* [e] *RRC (Kurchatov), RU-123182 Moscow, Russia* [f] *Joint Institute for Nuclear Research, RU-141980 Dubna, Russia* [g] *Oak Ridge National Laboratory, Oak Ridge, Tennessee 37831-6372, USA* [h] *University of Jammu, Jammu 180001, India* [i] *University of Münster, D-48149 Münster, Germany* [j] *SUBATECH, Ecole des Mines, Nantes, France* [k] *Gesellschaft für Schwerionenforschung (GSI), D-64220 Darmstadt, Germany* [l] *Universiteit Utrecht /NIKHEF, NL-3508 TA Utrecht, The Netherlands* [m] *University of Lund, SE-221 00 Lund, Sweden* [n] *University of Tsukuba, Ibaraki 305, Japan* [o] *Nuclear Physics Institute, CZ-250 68 Rez, Czech Rep.* [p] *KVI, University of Groningen, NL-9747 AA Groningen, The Netherlands* [q] *Institute for Nuclear Studies, 00-681 Warsaw, Poland* [r] *MIT Cambridge, MA 02139, USA* [s] *Institute of Physics, Bhubaneswar 751005, India* [t] *University of Tennessee, Knoxville, Tennessee 37966, USA*

*Invited talk at the Quark Matter '97, Tsukuba, Japan, 1-5 Dec 1997

Disoriented Chiral Condensates (DCC) have been predicted to form in high energy heavy ion collisions where the approximate chiral symmetry of QCD has been restored. This leads to large imbalances in the production of charged to neutral pions. Sophisticated analysis methods are being developed to disentangle DCC events out of the large background of events with conventionally produced particles. We present a short review of current analysis methods and future prospects.

1. Introduction

The QCD phase transition from normal hadronic matter to the Quark-Gluon-Plasma (QGP), in case of high energy heavy ion collisions, manifests itself in two forms: (1) Deconfinement transition and (2) Chiral symmetry restoration. One of the interesting consequences of the chiral transition is the formation of a chiral condensate in an extended domain, such that the direction of the condensate is misaligned from the true vacuum direction. This is called the formation of Disoriented Chiral Condensates (DCC). It has been proposed that the decay of the DCC domains would lead to large imbalances in the production of charged to neutral pions. The task for experimentalists is to carefully measure the number of neutral and charged pions as well as study their spectra. The challenge is to design sophisticated analysis tools on an event-by-event basis to identify DCC amidst the large background due to conventionally produced particles.

The formation of DCC domains has been proposed by Anselm[1], by Blaizot and Krzywicki[2] and by Bjorken, Kowalski and Taylor[3] in the context of high energy hadronic collisions in order to explain the puzzling Centauro and anti-Centauro type of events observed by cosmic ray experiments[5]. Bjorken et al.[3,6] proposed the so called "Baked Alaska" model which suggests that in case of hadronic collisions a hot fireball is produced with cold interiors having anomalous chiral order parameter. Rajagopal and Wilczek[4] were the first ones to discuss the DCC phenomena in the context of heavy ion reactions. They have suggested that the nonequilibrium dynamics during the chiral symmetry breaking phase transitions in case of heavy ion collisions may produce DCC domains. There is tremendous progress [6–12] in terms of theoretical understanding of DCC since then starting with different formalisms.

In the framework of the linear sigma model the Lagrangian can be expressed in terms of the order parameter $\Phi \equiv (\sigma, \vec{\pi})$, which is a combination of the scalar field σ and the pion field $\vec{\pi}$. At low temperatures the chiral symmetry is spontaneously broken. The potential, $V(\Phi)$, has a minimum in the sigma direction and all the direction of $\vec{\pi}$ are equally populated. Thus the distribution of neutral pion fraction defined by

$$f = \frac{N_{\pi^0}}{N_{\pi^0} + N_{\pi^+} + N_{\pi^-}} \tag{1}$$

is a gaussian with a mean of 1/3. This leads to the isospin symmetry of pions. As the system goes through the chiral transition and then rapidly expands and cools, it may roll down from the unstable local maximum of $V(\Phi)$ to the nearly stable values of one of the pion directions. The field will have to eventually settle in to the true ground state, but oscillations will continue for sometime which leads to amplification of soft pion modes. This effectively creates a cluster of low p_T pions in a correlated region (of a so called DCC

domain) with the probability of the neutral pion fraction given by:

$$P(f) = \frac{1}{2\sqrt{f}} \tag{2}$$

As is evident from this discussion, pions from a DCC domain will be emitted at low p_T and will have a distinct distribution pattern compared to the normal pion production mechanism without DCC.

Our ability to detect DCC domains depends on the number of domains, size of domains and number of DCC pions emitted from the domains. If the number of domains is more than one, then the distribution given by (2) gets modified, and for a large number of uncorrelated small domains, the resulting distribution becomes gaussian. The size of a DCC domain and the energy content determine the number of DCC pions. Clearly the fewer the number of domains and larger the number of emitted pions, the easier it is to detect in the laboratory. In addition, the probability of DCC formation in a nuclear collision at a given energy is important for the observation of DCC.

The cleanest evidence for the DCC formation can be obtained by precision measurement of N_{π^0} and $N_{\pi^\pm}$, or equivalently, N_γ and $N_{\rm ch}$ distributions. This assumes all charged particles are pions and all photons come from π^0 decays. In this manuscript we will deal mostly with analysis of neutral and charged particle distributions. Other signals which have been proposed for detection of DCC will be discussed towards the end of the manuscript.

2. Accelerator Experiments

The observation of centauro type of events have attracted lot of attention since the early 80's. Several accelerator experiments have been performed to search for such unusual events even before the concept of "DCC" came into being. The UA1 and UA5 experiments at the CERN-SPS have carried out search for centauros in $p-\bar{p}$ collisions at CM energies of 540 and 900 GeV, respectively, whereas DØ and CDF experiments at Fermilab have performed this search for CM energy of 1.8 TeV. These experiments have used the technique of the asymmetry of hadronic to electromagnetic energies. So far there is no evidence of any centauro type of events from these experiments.

Below we describe two current experiments for DCC search: the Minimax experiment for $p-\bar{p}$ collisions and the WA98 experiment for heavy ion collisions. Results from WA98 experiment will be discussed in detail. Other experiments at CERN-SPS such as NA45 and NA49 have plans for DCC search in near future.

2.1. Minimax Experiment at Fermilab

The Minimax Experiment[13] at Fermilab Tevatron is designed by Bjorken et al. for the DCC search in $p-\bar{p}$ collisions of 1.8TeV in the far forward region. The experiment is located at the CØ interaction region of the Tevatron and has been designed to measure the ratio of charged to neutral pions produced at pseudo-rapidities near 4.1. The lego acceptance of the detector is a circle of radius 0.65 units in η.

The data analysis for DCC search in Minimax is complicated because of small acceptance of the detector and various efficiency factors which come into play. The method

of normalized factorial moments has been utilized successfully to construct a set of "robust observables" which eliminate most of these effects [13]. This method is described in section 5.3. The results from these data is consistent with no DCC production mechanism.

2.2. WA98 Experiment at CERN-SPS

The WA98 experiment[14] at CERN-SPS emphasizes on high precision, simultaneous measurement of both hadrons and photons. The experimental setup consists of large acceptance hadron and photon spectrometers, detectors for charged particle and photon multiplicity measurements, and calorimeters for transverse and forward energy measurements. At present our search is limited to detailed event-by-event analysis of photon distributions from the Photon Multiplicity Detector and charged particles from Silicon Pad Multiplicity Detectors. Details of these detectors may be found elsewhere, here we give the essential points necessary for our present discussion.

The Photon Multiplicity Detector (PMD)

The PMD consists of a $3X_0$ thick lead converter sheet in front of an array of 54,000 pads, and is located at a distance of 21.5 meters from the target. Signals from several neighboring pads are combined to form clusters, characterized by the total ADC content and the hit positions. A threshold of 3 MIPs on the preshower ADC content gives an average photon counting efficiency in the range of 70%-75% depending on the centrality, with about 32% contamination due to showering hadrons. Thus the measured particle clusters, called "γ-like clusters" contain mostly photons together with a sizable contribution of charged pions.

The Silicon Pad Multiplicity Detector (SPMD)

The SPMD is located at 32.8 cm from the target. It is based on a double metal, AC coupled design consisting of approximately 4000 pads, arranged radially with 180 $\phi-$bins and 22 equal$-\eta$ bins between $\eta = 2.35$ and 3.75. The granularity of the detector is high enough that we have only $15 - 20\%$ occupancy in the highest multiplicity events. The efficiency of detecting a charged particle in the active area has been determined in a test beam to be 99%. Conversely the detector is transparent to high energy photons, since only about 0.2% are expected to interact in the silicon.

3. DCC Analysis Methods

Most of the DCC analyses so far are based on studying the fluctuations in neutral and charged particle measurements. Various analysis methods are being employed to characterize unusual events which show up beyond the statistical fluctuations. All the analysis in WA98 are being carried out in *event-by-event* basis. Current techniques in DCC analysis are the following:

- Global event characteristics: This analysis is performed by using the total number of photons and charged particles over the entire phase space covered by the photon and charged particle detectors.

- Methods for DCC domains localized in phase space: The available phase space is divided into several $\eta - \phi$ bins. Here we mention two of the analysis methods which

are sensitive enough to single out localized domains:

- Wavelet Analysis: This multiresolution analysis has the capability to scan the entire phase space. No averaging over events or $\eta - \phi$ space is done.
- Moments analysis: Various moments and combinations of those are calculated from the distribution of photons and charged particles in each bin.

In all these analysis, data are not corrected for detector effects and other efficiencies. Instead we compare the data with MC simulations which incorporates all known detector and physics effects. The output of VENUS 4.12 event generator is passed through a full simulation of our experimental setup using the GEANT 3.21 package from CERN. The same method of analysis is followed for both data and MC generated events. The idea is to look for

- shapes of different distributions: non-gaussian shapes in case where gaussian is expected and differences in various distributions in case of data and MC simulation
- exotic events: in case the shape is deviating from what is expected, one can study the events which show up beyond some predetermined limit.

4. Global Event Characteristics

The method of global event characterization in terms of the photon and charged particle multiplicity distributions over the full available phase space is suitable for the search of single large size DCC domain. The idea here is to look for events which fall far beyond the correlation line of these two distributions. For the current study we have assumed that the DCC could be formed only in central collisions. We will concentrate on the 10% most central events, defined by a measured transverse energy of at least 300 GeV in $3.5 < \eta < 5.5$.

In Figures 1a and 1b we present the minimum-bias multiplicity distribution for γ-like clusters and charged particles. The central data sample is shown by filled circles in these two figures. After all cuts are applied, there are 212646 events in this sample. A comparison with the MC simulation events chosen by identical cuts for central events is shown by the histogram.

The correlation between the charged and neutral multiplicities is presented on the right side of Figure 1 with the minimum bias distribution outlined, the central MC simulated events hatched, and the central data events shown as scattered points, each point corresponding to a single event. A strong correlation is seen between charged and neutral multiplicities, which suggests a more appropriate coordinate system with one axis being the measured correlation axis and the other perpendicular to it. This is represented by the Z axis and the D_Z axis as shown in figure 1b. We have chosen to work with the scaled variable $S_Z \equiv D_Z/\sigma_{D_Z}$ in order to compare relative fluctuations at different multiplicities. S_Z distribution for the data is shown as filled circles in figure 2(a).

4.1. DCC simulation

To estimate the effect of DCC production we have modified the output of VENUS events to include characteristic fluctuations in the relative production of charged and neutral pions. We assume that only a single domain of DCC is formed in each central

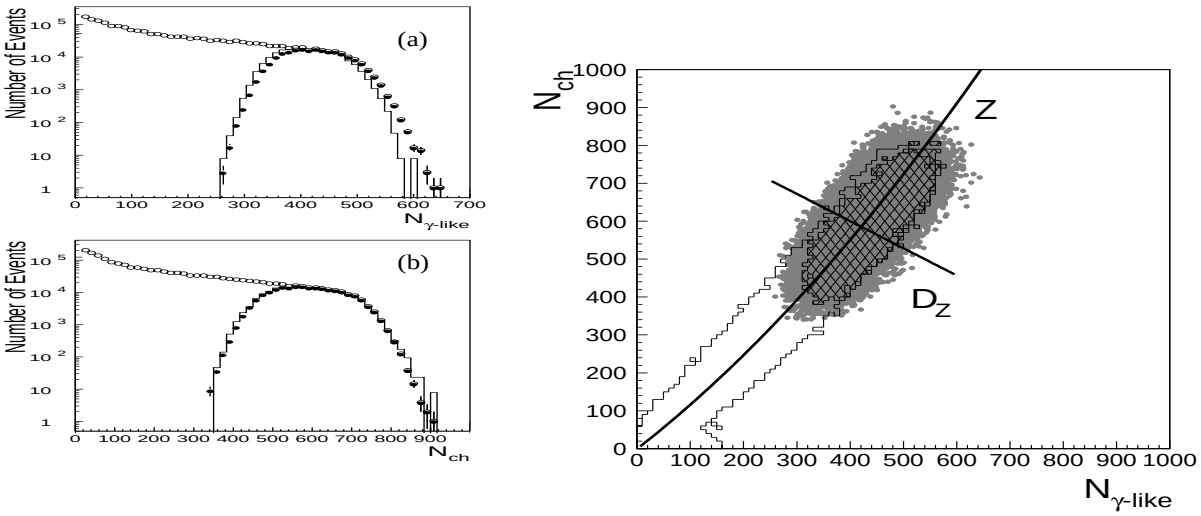

Figure 1. Multiplicity distributions of (a) γ-like clusters and (b) charged particles for minimum-bias (open circles) and central events (filled circles). The histograms show MC simulation results for central events. The right hand panel shows the correlation of $N_{\gamma-\text{like}}$ and N_{ch} for central events. The hatched region is for MC simulation results.

collision. A certain fraction, ζ, of the VENUS pions is associated with this domain and a value of f is chosen randomly according to the distribution shown in equation 2. Then the charges of the pions are interchanged pairwise ($\pi^+\pi^-$ or $\pi^o\pi^o$) until the charge distribution matches the chosen value of f. This simulates a DCC accompanied by the normal hadronic background in a way that conserves energy, momentum, and charge. The S_Z distribution for the $\zeta = 0\%$, 25% and 60% DCC hypotheses are shown in figure 2. The distributions get wider as ζ is increased. Thus DCC events would appear as outliers with respect to the bulk of the data.

4.2. DCC upper limit

We expect the DCC events to show up as non-statistical tails in the S_Z plot. Since we do not see no such events in our data sample, we are faced with the possibilities that single-domain DCCs are very rare, very small, or both. To check which hypotheses are consistent with our data, we determine upper limits on the frequency of DCC production as a function of its size, as represented by ζ.

We have calculated the 90% confidence limits for two scenarios and the results are shown in the right side of figure 2. The first, shown as the solid line, is based upon the conservative assumption that the MC simulation should describe the data perfectly in the absence of a DCC signal. The second scenario, shown as the dashed line, assumes that the difference between the data and VENUS is due to detector effects and that the widths should be the same. Further details can be found in [16].

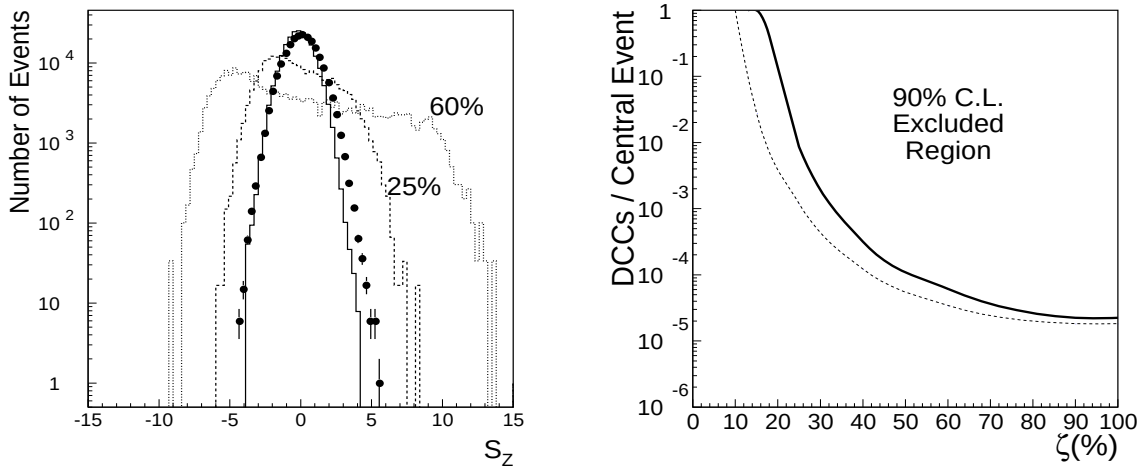

Figure 2. (a) S_Z distribution for the experimental data is shown, overlaid with simulation results incorporating 0%, 25% and 60% DCC in every event. (b) 90% C.L upper limit on DCC production per central event as a function of the fraction of DCC pions under two assumptions.

5. Methods for DCC domains localized in phase space

The localized DCC analyses take advantage of the predictions that the coherent fluctuations caused by DCC tend to cluster in phase space. A similar analysis technique that described in the last section can be used in small phase space. Here we describe two other analysis methods, *viz.*, use of wavelets and factorial moments.

In WA98, the localized analysis is done by taking the data of the full overlap regions of PMD and SPMD, which lies between $\eta = 2.8$ and 3.75. In figure 3 this zone is shown for a single event in terms of $x - y$ phase space distribution on the PMD plane. Open circles show the distribution of γ-like clusters from PMD and filled circles show the charged particle distributions from SPMD projected on to PMD plane. The neutral and charged particle distributions are evenly distributed in this event. The methods discussed below are sensitive to single out exotic events out of a large data sample.

5.1. DCC simulation for localized analysis

For the simulation of normal background events we have adopted the same simulation method as described in section 3 whereas the DCC simulation is done differently compared the global case. Since the localized methods are sensitive to smaller phase space zones, we have the option of introducing single or multiple domains of varying sizes to any phase space into the simulation and carry out further analysis. For the present study, we have chosen a DCC domain to be within $3 \leq \eta \leq 4$ and $0 \leq \phi \leq 90$. The common phase space of PMD and SPMD overlaps with this choice of domain. The rest of the analysis follows as described in section 4.1 including the full GEANT simulation of WA98 detectors.

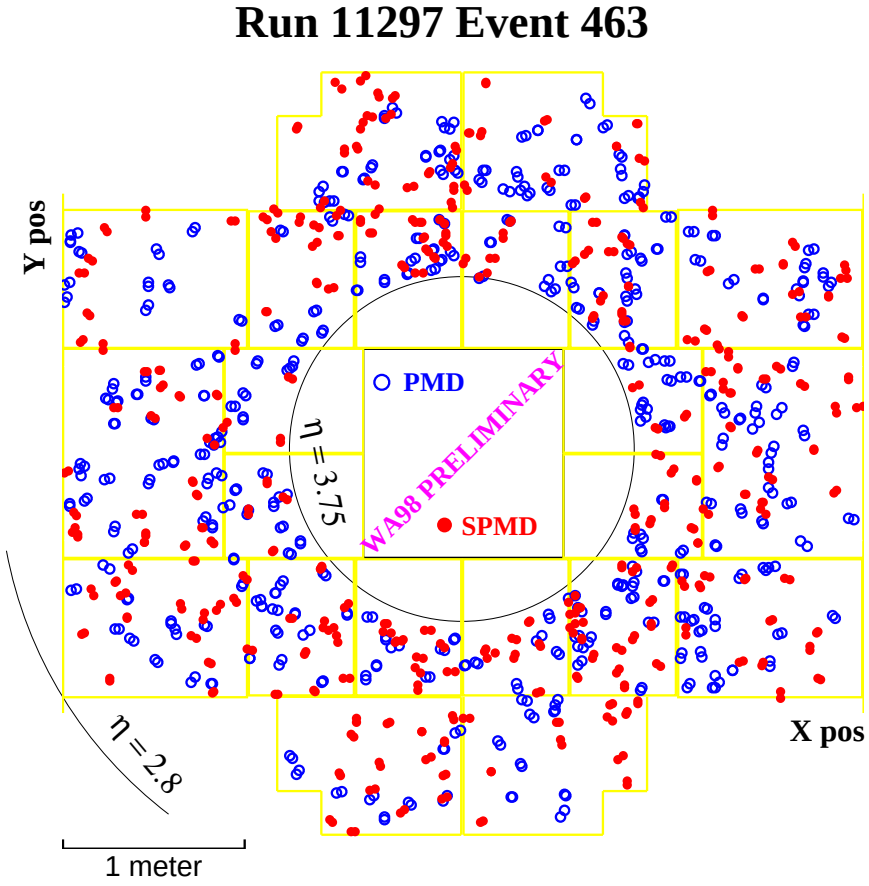

Figure 3. $x-y$ phase space distribution of a normal event from the WA98 experiment on Pb+Pb reactions at 158·A GeV/c.

5.2. Wavelet Analysis

A unique analysis method based on the discrete wavelet transformation (DWT) is adopted to search for the fluctuation in neutral pion fraction in a localized $\eta-\phi$ space. This method was first proposed by Huang et al.[17] for DCC search. Wavelets are the basis functions in some representations of arbitrary functions that satisfy certain requirements like invertibility, orthogonality etc. (as sines and cosines in case of Fourier transformation). These arbitrary functions can be functional representations of a given data set. The most interesting feature of the discrete wavelet transformation is the zooming action at each location of the various resolution scale. Due to the completeness and orthogonality of the DWT basis, there is no information loss at any scale.

In our present analysis, we have chosen the arbitrary function to be the neutral pion fraction given in equation (1). The DWT representation of the neutral pion fraction can be represented by,

$$f^{(j)}(x) = \sum_{k=0}^{2^{j-1}-1} f_{j-1,k}\phi_{j-1,k}(x) + \sum_{k=0}^{2^{j-1}-1} \tilde{f}_{j-1,k}\psi_{j-1,k}(x) \tag{3}$$

where $f_{j,k}$ are the mother function coefficients (MFC) and $\tilde{f}_{j,k}$ are the father function coefficients (FFC) at position index k of resolution scale j. The MFC's and FFC's are

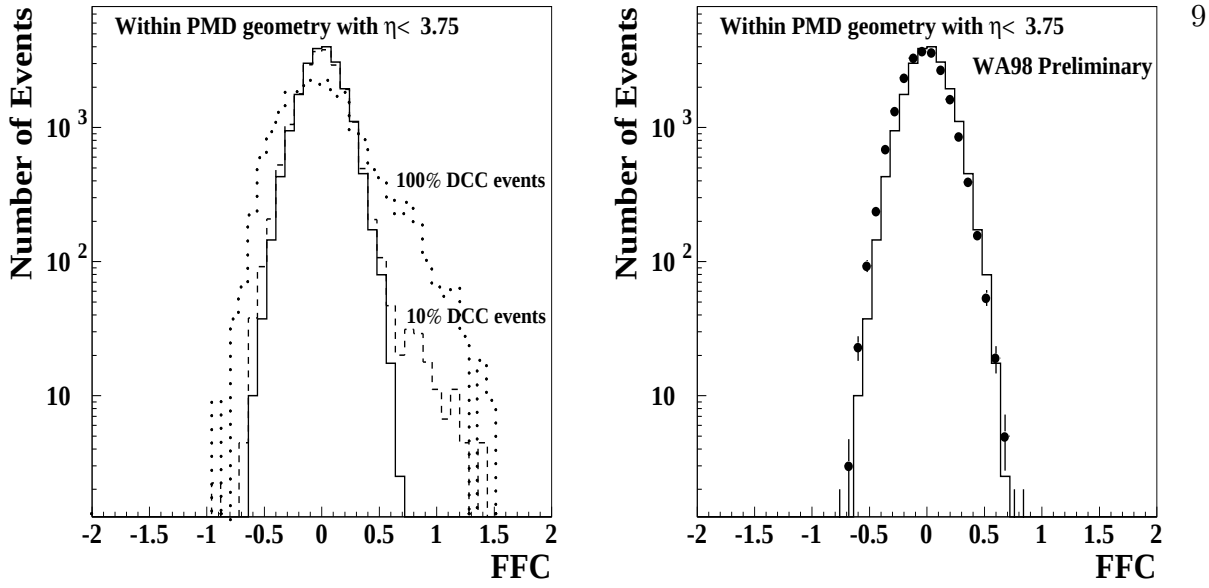

Figure 4. (a) FFC distribution of simulated data of different percentage of DCC events. (b) FFC distribution of data and comparison with MC simulation.

the carriers of information at each scale. In Haar basis, MFC's are the average between two bins and FFC's are the half difference between two bins. The variable x can be η, ϕ or a combination of both η and ϕ. We have chosen x to be η in our case. $\phi(\eta)$ and $\psi(\eta)$ are called the mother and father functions, respectively. In the present analysis we have used D-4 wavelet basis.

In order to verify if the FFC distributions are sensitive to events with DCC pions we have carried out the MC simulation described above for different percentage of DCC events present in the full sample. We show two of these cases in figure 4(a). The solid histogram shows the FFC distribution at $j = 2$ in the absence of any DCC event. This is our background simulation. The dotted and dashed curves represent the cases where DCC events are present in all the (100%) events and 10% of the events, respectively. In all cases the DCC domain is chosen to be the same, as described in previous section. Significant difference between the background histogram and events with DCC can be seen here. In this method one is sensitive to a small admixture of DCC events in the full sample. It is seen that even if the occurrence of DCC events compared to the total number of events is very less, still then there are significant number of events beyond 3σ of FFC distribution of background events at j=1. These events are to be tagged and studied in detail for the presence of DCC.

The WA98 data FFC distribution (at $j = 2$) for central events is shown as solid points in figure 4(b) and overlaid on the top is the background MC simulation. Data and simulation match quite well. Detailed analysis is in progress by rotating the full phase space by a given angle in ϕ and repeating the whole analysis. Another way is to rotate the SPMD plane with respect to PMD plane and determining FFC from the resulting distribution.

Another interesting quantity in the fluctuation analysis at each scale is the wavelet power spectrum, defined as:

$$P_j = \frac{1}{2^j} \sum_{k=0}^{2^j-1} \mid \tilde{f}_{jk} \mid^2 . \qquad (4)$$

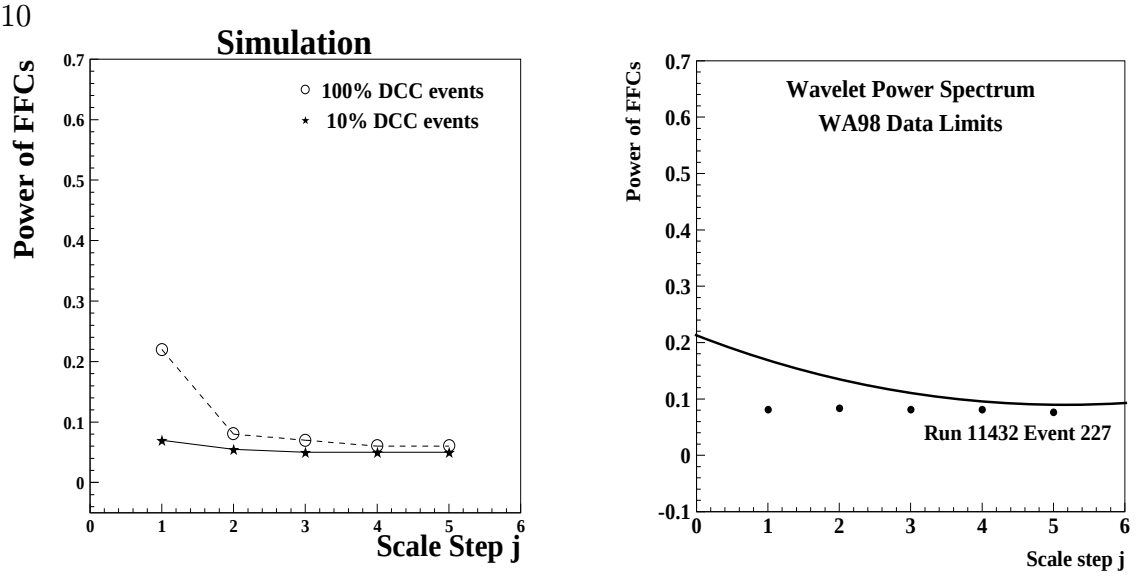

Figure 5. (a) Wavelet power spectrum from simulated MC events for different percentage of DCC events (b) Power spectrum for WA98 data. Events beyond the three sigma value of background MC simulation are to be selected as DCC candidates for further study.

Figure 5(a) shows the power spectrum calculation for different cases. The power spectrum for background MC simulated events is quite flat at all scales, j. In the left hand panel for figure 5 we show simulation for 100% and 10% DCC events. In these cases we are averaging over many events which is making the P_j very weak. That means, P_j at j=1 which is so much higher for 100% DCC events has gone down below noticeable level for 10% DCC. Instead of averaging over events which kills the signals this plot will be presented event-by-event.

One can filter out significant number of exotic events by selecting the events which have FFC beyond the three sigma level of the fitted gaussian of the solid curve of figure 5(b). The power spectrum corresponding to the three sigma value of FFC is shown in the right panel of the figure as a solid curve. The selected events will have a power value above this line. These events, once found, have to be analyzed further by looking at $\eta - \phi$ or $x - y$ event display plots for the existence of DCC.

5.3. Bivariate Moments

Since pions from the DCC domains would appear as localized fluctuations in the joint charged to neutral particle distributions, one of the elegant analysis methods is to calculate *bi-variate factorial moments* such as:

$$f_{1,0}(ch,\gamma) = \langle N_{ch} \rangle, \qquad f_{0,1}(ch,\gamma) = \langle N_{\gamma} \rangle,$$
$$f_{1,1}(ch,\gamma) = \langle N_{ch} N_{\gamma} \rangle, \qquad f_{2,0}(ch,\gamma) = \langle N_{ch}(N_{ch}-1) \rangle \tag{5}$$

and so on. Here the averaging is done over a large number of samples. Filtering of true fluctuations from the above distributions become quite complicated because of various detector effects, efficiency and background factors. Some of the deficiencies could be overcome by using the generating function technique [18] which can be applied to concerned distributions. In that way we can evaluate normalized factorial moments for the distributions which have the ability to filter out the non-statistical fluctuations from the envelop

of statistical noise. One defines the *normalized bi-variate factorial moments* as:

$$F_{i,j} = \frac{f_{i,j}}{f^i_{1,0} f^j_{0,1}} = \frac{\langle N_{ch}(N_{ch}-1)\ldots(N_{ch}-i+1)\ N_\gamma(N_\gamma-1)\ldots(N_\gamma-j+1)\rangle}{\langle N_{ch}\rangle^i \langle N_\gamma\rangle^j} \ , \tag{6}$$

One defines the ratios of these factorial moments as:

$$R_{i,1} = \frac{F_{i,1}}{F_{i+1,0}} \tag{7}$$

The Minimax collaboration has shown that these ratios are not affected by detector effects or efficiencies, and termed as "Robust Observables". Here the sampling is done over total number of events, rather than event-by-event. These ratios yield 1 for generic distributions and 1/(i+1) for pure DCC.

In case of WA98 data the these observables are not robust, but one can calculate these quantity in case of both simulation with and without DCC and then compare with data. In order to make these quantities suitable for identifying single event fluctuations the averages are taken over a considerable number of $\eta - \phi$ phase space bins of N_γ and $N_{\rm ch}$. This can be studied in WA98 because of the large acceptance of both photon and charged particle detectors. In average, the results from the data match with MC simulation. Detailed analysis is in progress to sort out events with large fluctuations.

6. Future Prospects

First we outline some of the new analysis from WA98 experiment by combining with neutral and charged particle spectra. Photon and charged particle momentum spectra for different event classes based on $N_{\gamma-{\rm like}}$ and $N_{\rm ch}$ distributions (e.g., by choosing events around the mean value of FFC and events far from the mean) may show significant differences since DCC pions are predominantly of low p_T. Average p_T of photons obtained from PMD may also show differences for these event classes.

Several other signals of DCC have been discussed in the literature for the detection of DCC. It has been proposed that the photon and dilepton signals will be significantly enhanced in the presence of DCC. This has been discussed by V. Koch and by J. Randrup in this conference. M. Asakawa has argued (also in this conference) that non-central collisions may be a better place to look for DCC. The two particle correlation (HBT) effect may also be suppressed if a large domain forms [8]. Another interesting signal may be the enhancement in the production of baryons and antibaryons [19].

Most of the future experiments at RHIC and LHC have plans to search for the signals of DCC. A highly granular photon multiplicity detector is being planned for the STAR experiment at RHIC, which, in combination with charged particle detectors and FTPC, will be quite adequate for DCC search. Here one would be able to select on the low p_T particles, characteristic of DCC pions. DCC search in PHENIX will be possible by correlating signals from charged particle detectors and photons from EMCAL. The PHOBOS experiment, with its large acceptance charged multiplicity detector, will be able to search for unusual fluctuations in the production of charged particles. The fluctuations can then be correlated to the production of very low p_T hadrons measured in its two arm spectrometer. The BRAHMS experiment is considering to add a photon arm to look for

DCC. A Photon Multiplicity Detector similar to that of STAR is proposed to be included in the ALICE experiment at LHC, which along with charged particle detectors will be able to search for DCC.

7. Summary

The phenomenon of DCC is quite interesting, its observation in heavy ion collisions would signal the chiral transition as well as bring a wealth of information for understanding of QCD. Since the hope is for such transition to occur at RHIC and LHC energies, we have to be well equipped with precision measurement tools and sophisticated analysis methods. In this article we have outlined a list of analysis methods that exist at present with a speculation on other signals and new techniques for future. With continued development and understanding in theoretical aspects and analysis tools, one would hope for the best to come from the new data from the upcoming experiments.

TKN acknowledges very fruitful discussions with Krishna Rajagopal, Jorgen Randrup, Ajit Srivastava and Xin-Nian Wang.

REFERENCES

1. A.A. Anselm, M.G. Ryskin, Phys. Lett. **B266**, (1991), 482.
2. J. -P. Blaizot and A. Krzywcki, Phys. Rev. **D46** (1992) 246.
3. J.D. Bjorken, Int. J. Mod. Phys. **A7**, (1992), 4189; J.D. Bjorken, K.L. Kowalski, C.C. Taylor, "Baked Alaska", SLAC-PUB-6109, Apr., 1993.
4. K. Rajagopal, F. Wilczek, Nucl. Phys. **B399**, (1993), 395.
5. Proceedings of VIII International Symposium on Very High Energy Cosmic Ray Interactions (Tokyo, Japan), 24-30 July 1994; C.M.G. Lattes, Y. Fujimoto, and S. Hasegawa, Phys. Rep. **65**, (1980), 151; J. Lord and J. Iwai, International conference on HEP (Dallas, 1992)
6. J.D. Bjorken in hep-ph/9712434.
7. S. Gavin, Andreas Gocksch, Robert D. Pisarski, Phys. Rev. Lett. **72** (1994) 2143.
8. S. Gavin, Nucl. Phys. A590 **176** (1995) 163.
9. Jorgen Randrup, Nucl. Phys. **A616** (1997) 531.
10. Jorgen Randrup and Robert L. Thews, hep-ph/9705260.
11. Masayuki Asakawa, Zheng Huang, Xin-Nian Wang, Phys. Rev. Lett. **74** (1995), 3126.
12. Krishna Rajagopal, "The Chiral Phase Transition in QCD: Critical Phenomena and Long Wavelength Pion Oscillations", appeared in Quark-Gluon Plasma 2, edited by R. Hwa, World Scientific, 1995; and Krishna Rajagopal in hep-ph/9703258.
13. T.C. Brooks et al. (Minimax Collaboration), hep-ph/9609375, J.D. Bjorken et al., hep-ph/9610379.
14. B. Wyslouch et al., The WA98 Collaboration, these proceedings.
15. M.M. Aggarwal et al., The WA93 Collaboration, Nucl. Instr. Meth. **A372** (1996) 143.
16. M.M. Aggarwal et al., The WA98 Collaboration, to be published in Phys. Lett. B.
17. Zheng Huang et al., Phys. Rev. **D54** (1996) 750.
18. E. A. DeWolf, I. M. Dremin, W. Kittel, Phys. Rep. 270: 1 (1996).
19. J.I. Kapusta and A.M. Srivastava, Phys. Rev. D **52** (1995) 2977.